International Journal of Pharmaceutics 406 (2011) 21–30

Contents lists available at ScienceDirect

International Journal of Pharmaceutics

journal homepage: www.elsevier.com/locate/ijpharm

NP-647, a novel TRH analogue: Investigating physicochemical parameters critical for its oral and parenteral delivery

Kailas Khomane[a], Lokesh Kumar[a], Chhuttan Lal Meena[b], Rahul Jain[b], Arvind Bansal[a,*]

[a] Department of Pharmaceutics, National Institute of Pharmaceutical Education and Research (NIPER), Sector-67, S.A.S Nagar, Mohali, Punjab, India
[b] Department of Medicinal Chemistry, National Institute of Pharmaceutical Education and Research (NIPER), Sector-67, S.A.S. Nagar, Mohali, Punjab, India

ARTICLE INFO

Article history:
Received 22 September 2010
Received in revised form
13 December 2010
Accepted 17 December 2010
Available online 24 December 2010

Keywords:
Preformulation
Consensus approach
Physicochemical properties
TRH analogues
Dissolution titration template
Peptide delivery

ABSTRACT

NP-647 (L-pGlu-(2-propyl)-L-His-L-ProNH$_2$) is a novel thyrotropin releasing hormone (TRH) analogue, with potential antiepileptic activity. In the present study, the physicochemical parameters of NP-647, including its solid state properties, dissociation constant, partition coefficient, solubility (intrinsic solubility and pH-solubility profile) and stability (gastrointestinal enzymatic stability, pH-stability profile and temperature stability) were investigated for their criticality for oral and parenteral delivery. NP-647 was characterized as amorphous material having glass transition temperature of 66.73 °C at 50% RH. It was found very hygroscopic with deliquescent in nature. pK_a of the compound, as determined using potentiometric titration, was found to be 7.2 ± 0.02 (basic). Intrinsic solubility and pH-solubility behavior were determined using dissolution titration template method. NP-647 has intrinsic solubility of 2.4 ± 0.01 mg mL^{-1}. Partition/distribution studies indicate that NP-647 has a low log P (−1.07 ± 0.06) and log $D_{7.4}$ (−1.20 ± 0.02), characteristic of hydrophilic molecule. It was found most stable in tartrate buffer of pH of 5.0. Arrhenius plot of NP-647 suggest its half life of ∼3.2 years and shelf life of ∼6 months. These studies conclude that amorphous nature of NP-647 with deliquescent property will be critical in its solid oral dosage formulation and need to be investigated further.

1. Introduction

Thyrotropin-releasing hormone (L-pGlu-L-His-L-ProNH$_2$; TRH) is a tripeptide, synthesized in the hypothalamus and acts in the anterior lobe of pituitary gland to control the release of TSH (thyroid stimulating hormone) (Griffith, 1985). Neuro-pharmacological studies on TRH reported its potential use in treatment of central nervous systems (CNS) disorder, including Huntington's chorea (Spindel et al., 1981), schizophrenia (Nemeroff et al., 1984), Alzheimer's disease (Albert et al., 1993), epilepsy (Jaworska-Feil et al., 2001; Kubek and Garg, 2002; Tsuboyama et al., 1992), depression (Lafer et al., 1993) and brain/spinal injury (Takeuchi et al., 1994). However, its short half life, poor selectivity, along with cardiac and endocrine side effects severely limit its utility as an effective neuropharmacological agent (O'Leary and O'Connor, 1995). Several TRH analogues have been investigated to overcome these limitations. Most of the reported analogues, however, suffer from a poor access across blood brain barrier, instability in plasma, undesirable endocrine activity and a poor selectivity toward TRH R2 receptor, primarily responsible for its neuropharmacological action (Heuer et al., 2000; Sun et al., 2003, 2009).

NP-647 (L-pGlu-(2-propyl)-L-His-L-ProNH$_2$) (Fig. 1) is a novel TRH analogue, synthesized by substituting C-2 position of the imidazole ring of histidine amino acid of TRH with propyl group (Jain et al., 2006; Kaur et al., 2007; Rajput et al., 2009). Receptor-binding studies exhibited its 12 folds selectivity toward the TRH-R2 receptor, present predominantly in brain stem and spinal cord region, responsible for its neurophysiological function (Kaur et al., 2005). Preclinical and safety pharmacology studies of NP-647 showed an antiepileptic activity without significantly altering the plasma thyroid stimulating hormone (TSH) levels and mean arterial blood pressure, thereby suggesting its selective central activity, without any associated hormonal and cerebrovascular system effects (Rajput et al., 2009). These studies demonstrated the potential of NP-647 as an antiepileptic agent, devoid of undesirable hormonal side effects.

Delivery of a molecule is very crucial in clinical development of NCEs and physicochemical properties of a molecule play critical role in its delivery. In case of peptide molecules, aqueous solubility, pH-stability profile, and temperature stability are critical parameters for its parenteral delivery. Oral delivery of peptides is more challenging. Solid form (amorphous/crystalline), gastrointestinal stability (peptide undergo enzymatic or chemical hydrolysis in GIT), permeability (mostly peptides are hydrophilic in nature and are poorly absorbed by passive diffusion; however they may cross membrane by carrier mediated mechanism) and hygroscopicity

* Corresponding author. Tel.: +91 172 2214682; fax: +91 172 2214692.
E-mail address: akbansal@niper.ac.in (A. Bansal).

0378-5173/$ – see front matter © 2010 Elsevier B.V. All rights reserved.
doi:10.1016/j.ijpharm.2010.12.025

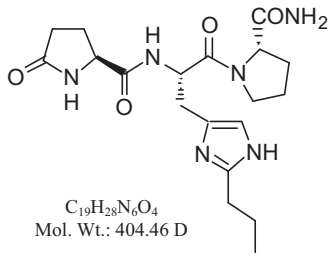

Fig. 1. Chemical structure of NP-647 (L-pGlu-(2-propyl)-L-His-L-ProNH$_2$).

(crucial in solid oral dosage form) of a molecule govern its oral delivery. Hence the present work deals with physicochemical characterization of NP-647 which includes solid state characterization, determination of different solubility parameters (ionization, solubility, and lipophilicity), gastrointestinal stability, pH-stability profile, and temperature stability. This shall enable a thorough understanding of the preformulation profile of NP-647 and its implications on drug development.

2. Materials and methods

2.1. Chemicals

NP-647 was synthesized in the Department of Medicinal Chemistry, NIPER-SAS Nagar (India) using solution phase peptide synthesis. Methanol and acetonitrile (HPLC grade) were purchased from J. T. Baker (USA). Sodium salt of octansulfonic acid, 0.5 N hydrochloric acid (HCl), sodium hydroxide (NaOH) titrisol®, phosphoric acid, potassium phosphate (monobasic), potassium phosphate (dibasic) and n-octanol were purchased from Merck (Germany). Potassium hydrogen phthalate and potassium chloride were procured from HiMedia laboratories (India) and RFCL limited (India) respectively. All the chemicals used for the experiments were of analytical grade. Ultrapure water was prepared using an ELGA (Bucks, UK) water purification unit.

2.2. Software programs

Physicochemical parameter like dissociation constant (pK_a), intrinsic solubility, and log P of NP-647 were predicted using various software programs. These included ACD/I-lab, v11.0 (ACD/I-Lab Service, Canada), Discovery Studio, v2.0 (Accelrys Inc., USA), Pallas, v2.0 (CompuDrug International, Hungary), VCCLAB (Virtual Computational Chemistry Laboratory, Germany) and ADME/Toxes, v3.5 (www.pharma-algorithms.com), SPARC (http://ibmlc2.chem.uga.edu), ChemSilico (www.chemsilico.com), Episuite (www.epa.gov), ChemOffice (www.cambridgesoft.com), ChemSpider (www.chemspider.com) software.

2.3. Chromatographic system

The chromatographic system (Shimadzu, Japan) consisted of LC-20AT pump fitted with a degasser unit DGU-20A5, a SIL-20AC auto sampler with refrigeration unit, SPD-M20A UV-Vis detector (PDA) and a CTO-10A VP column oven. The system was controlled by a CBM-20A system controller with Class VP chromatography software. Analysis was carried out using a reversed phase LiChrospher® 100 C8 analytical column (4.6 mm × 200 mm, 5 μm particles; Merck), preceded by a 3 mm × 4 mm C8 guard column (LichroCART®, Merck) maintained at 40 °C.

2.4. Insilico studies

The main objective of the *insilico* studies was the accurate prediction of physicochemical properties of NP-647.

"Consensus" was selected among the various prediction approaches, because of its much better performance than any other individual predictive model (Abshear et al., 2006). In this prediction approach 'a set of software programs' is used to predict the particular property of the compound. 'A set of software programs' usually consist of more than one different software programs which give similar prediction value of particular property for the same compound.

The best software program may give the worse prediction for the compound of interest and vice versa. This is because prediction performance of any software program depends on its "applicability domain" and how well the "descriptor(s)" correlate with the properties in question. If the compound in the question is similar to those used in the 'training set' of the program, then it is called to be in the applicability domain of that software. One should always check the applicability domain of the software before using it, but in case of commercial software programs applicability domains are not usually available. In such cases "read-across approach" is useful (Dearden and Worth, 2007).

In this approach, applicability of the software is judged by comparing predicted values of the same property for one or more similar compounds for which experimental values of the property are available. If predictions for "structurally related" compounds are acceptable, then we can assume that the prediction for the compound of interest, is also acceptable. Hence, to develop consensus, 'read-across approach' was used to screen the various software programs. In this case, TRH was selected as model drug, since it is the most similar to all the compounds to be screened (TRH analogues) and experimental values of its solubility parameters i.e., pK_a, log P and aqueous solubility are available in literature. Ten software programs (see Section 2.2) were screened through this approach. Of them, five (ACD/lab, Discovery studio, Pallas, ADME/Toxes, VCCLAB software) were selected for prediction of NP-647. By comparing predicted values of pK_a, log P/D, aqueous solubility, consensus based on average were developed and used for prediction.

2.5. Solid state characterization

2.5.1. X-ray powder diffractometry (XRPD)

XRPD patterns of samples were recorded at room temperature on Bruker's D8 advance diffractometer (Bruker, Germany) with Cu K_α radiation (1.54 Å), at 40 kV, 40 mA passing through nickel filter. Analysis was performed in a continuous mode with a step size of 0.01° and step time of 1 s over an angular range of 2–40° 2θ, using zero background holder. Obtained diffractograms were analyzed with DIFFRACplus EVA (version 9.0) diffraction software.

2.5.2. Thermogravimetric analysis (TGA)

The mass loss of sample as a function of temperature was determined using Mettler Toledo 851^e TGA (Mettler Toledo, Switzerland) operating with STAR^e software (version 9.0). About 4.5–5.0 mg of NP-647 was accurately weighted in open alumina crucibles and subjected to the thermal scan of 25–500 °C at the heating rate of 10 °C min^{-1} under dry nitrogen purge (20 mL min^{-1}). Prior to analysis calibration of the instrument was performed using Aluminium (Al).

2.5.3. Differential scanning calorimetry (DSC)

DSC analysis was performed using DSC, Model Q2000 (TA Instruments, USA) operating with Universal analysis® software (version 4.5A). About 4.5–5.0 mg of NP-647 was accurately weighted in

crimped aluminium pans and subjected to the thermal scan of 25–300 °C at the heating rate of 10 °C min^{-1}. The dry nitrogen purge was maintained at 50 mL min^{-1}. Prior to analysis calibration of the instrument was performed using high purity standards of zinc (Zn) and indium (In). Modulated DSC (MDSC) was also performed from 25 to 120 °C at 2 °C min^{-1} with modulation amplitude of 0.5 °C min^{-1} and a period of 60 s.

2.5.4. Microscopy

Microscopic studies were performed using the Leica DMLP polarized microscope (Leica Microsystems Wetzlar GmbH, Germany), equipped with Linkam LTS 350 hot stage. Photomicrographs of samples were acquired using JVS color video camera and analyzed using Linksys32 software. Samples were mounted on glass slides and observed under optical as well as polarized light. Also, samples were heated from 25 °C to 300 °C at a heating rate of 10 °C min^{-1} to observe any transitions.

2.5.5. Dynamic vapor sorption (DVS)

Gravimetric vapor sorption studies were carried using DVS, Model Q5000 SA (TA Instruments, USA) to understand hygroscopicity behavior of NP-647. For the same, 6.8 mg solid form was weighed in the sample pan and exposed to predetermine RH, using nitrogen as a carrier gas. The experiment was performed under isothermal condition at 25 °C. The humidity was varied in four cycles of sorption–desorption, viz., 25% → 0% (Desorption 1), 0% → 95% (Sorption 1), 95% → 0% (Desorption 2), and 0% → 95% (Sorption 2). The sample weight was recorded at the ramping rate of 5% RH throughout the experiment. The humidity was changed to the next step when the change of weight reached ±0.01 mg or after 30 min, whichever was later. Data was collected and exported to an Excel spreadsheet for graphing.

2.6. pK_a and solubility determination

2.6.1. pSOL instrument

pK_a and solubility were determined using pSOL instrument (pION Inc., USA). Experimental data was obtained using pD software and subsequently analyzed using pS software program. The pSOL instrument consists of a Gemini unit, pH electrode, serial conductors, dispenser tips, and reagent tubing. The Gemini unit is equipped with three dispensers (acid, base and water), capable of dispensing as small as 20 nL in a single step. The acid and base dispersers used a glass syringe of 500 μL capacity while water dispenser use 5 mL capacity glass syringe. pH electrode is a double junction silver/silver chloride glass electrode, quality controlled by the manufacturer. Potentiometric titrations were carried out at 25 ± 0.2 °C under the blanket of argon gas in a glass tube, which was housed in a thermostatic jacket. pD-software program of pSOL instrument suggest amount of the sample required for pK_a and solubility studies. Total volume of the titrated solution ranges from 1.7 to 17 mL, but in these studies it was less than 5 mL. All the titrations were carried out in presence of 0.15 M KCl to decrease the effect of small change in ionic strength due to sample and titrant addition. This background electrolyte also improves the electrode performance. Each experiment was performed in triplicate.

2.6.2. pK_a determination

pK_a of NP-647 was determined by potentiometric titration method using the pSOL instrument. It requires 'predicted pK_a values' as an input and simulates the entire titration curve before starting actual experiment. This 'simulated titration curve' served as a template and guides the instrument for collecting sampling point (pH measurements) during the course of titration curve. Titrations were performed using 0.5 M hydrochloric acid, and 0.5 M potassium hydroxide in a glass tube under the blanket of argon gas flow in solution containing 0.15 M potassium chloride at 25 ± 0.2 °C. Titration medium was continuously agitated with a teflon-coated magnetic stir bar. Method required less than 100 μg of drug and the experiment was carried out in triplicate. Refinement of obtained data was carried out based on goodness of fit (GOF) factor.

2.6.3. Solubility determination

Solubility of NP-647 was determined by the potentiometric acid–base titration using the pSOL instrument (Avdeef, 1998; Avdeef et al., 2000). This method of solubility measurement is based on the characteristic shift in dissociation constant (pK_a) values in presence of precipitate and is called as 'dissolution titration template' (DTT) method (Avdeef and Berger, 2001).

The pSOL instrument requires experimental or predicted log P and pK_a values as input parameters. The instrument calculates intrinsic solubility (S_o) from log P values using the Hansch expression (Eq. (1)) and uses this calculated S_o and pK_a to simulate the entire titration curve before initiating the assay.

$$\log\left(\frac{1}{S_o}\right) = 1.38\ \log P - 1.17 \tag{1}$$

This 'simulated curve' then serves as a template for actual experiment. Experimental procedure for solubility measurement is similar to that of pK_a determination. Three titrations were performed for solubility determination and the data obtained was refined using pS software program.

2.6.4. Theoretical biopharmaceutical parameters of NP-647

Rate limiting steps in the absorption of NP-647, was assessed by calculating parameters like dissolution time (T_{disso}), absorbable dose (D_{abs}) and dissolution number (D_n), using the following equations (Amidon et al., 1995) (Eqs. (2)–(4))

$$T_{disso} = \frac{h\rho r}{3DC_s} \tag{2}$$

where h is the diffusion layer thickness, ρ the is density of the material, r is the radius of particle, D is the diffusion coefficient and C_s is the solubility in mg mL^{-1}.

$$D_n = \frac{\text{MITT}}{T_{disso}} \tag{3}$$

where MITT is the mean intestinal transit time assumed to be 199 min.

$$D_{abs} = P_{eff}C_sA\,\text{MITT} \tag{4}$$

where P_{eff} is the effective permeability and A is the intestinal area.

2.7. Partition/distribution coefficient

2.7.1. Analytical method for log P/D determination

HPLC analysis was performed by injecting 20 μl of samples in C-8 column and purging with a mobile phase consisting of an acetonitrile: methanol: aqueous phase in the ratio of 15:15:70. Aqueous phase comprised of 0.05% octansulfonic acid sodium salt, pH 2.2 adjusted with phosphoric acid. The eluted compounds were detected at a wavelength of 197 nm using a PDA detector. Prior to analysis, mobile phase was filtered through 0.45 μm nylon membrane and degassed. HPLC method was validated according to the ICH guideline Q2(R1) with respect to linearity, precision, accuracy, specificity, limit of quantification, limit of detection and system suitability (ICH, 1996).

2.7.2. Partition/distribution coefficient determination

Under these studies, two constants, viz. partition coefficient (log P) and distribution coefficient (log $D_{7.4}$) were determined using the Micro-shake flask method (Ford et al., 1991; Rathore et al.,

2008). Aqueous phase for determination of partition coefficient and distribution coefficient were tris buffer (pH 9.0) and phosphate buffer (pH 7.4) respectively. In order to achieve a saturation state, high purity analytical grade n-octanol was shaken with a sufficient quantity of aqueous phase for 24 h on a mechanical shaker at 100 rpm and was allowed to stand till phase separation.

Accurately weighted NP-647 was added to water (1 mg mL^{-1}) pre-saturated with n-octanol, followed by sonication to dissolve the drug. Experiment was carried out in duplicate using three different volume ratios of 1:1 (1.5 mL each phase), 1:2 (1 mL octanol and 2 mL buffer) and 2:1 (2 mL octanol and 1 mL buffer). Volumetric flask (3 mL) was nearly filled by entire volume of the two phases to prevent the loss of the material due to volatilization. In order to achieve uniform dispersion of two phases, 15 piston strokes were applied to the partition medium using a 10 mL glass syringe and kept in shaker water bath maintained at 37 ± 1 °C for 3 h at 100 rpm. Separation of phases was achieved by centrifugation at 3000 rpm for 10 min. An aliquot of each of the phases was taken for analysis. HPLC analysis was performed in triplicate using above mentioned validated HPLC method. Eq. (5) was used to calculate the log *P* and log *D* values.

$$\log(P \text{ or } D) = \log\left(\frac{C_o}{C_{aq}}\right) \quad (5)$$

where C_o and C_{aq} were the concentrations of NP-647 in octanol and aqueous phases, respectively.

In order to confirm the establishment of partition equilibrium, analysis was performed after 12 h. There was no difference in partition coefficient of NP-647, indicating that period of 3 h was sufficient for equilibration. Care was taken to minimize the risk of including traces of n-octanol, while sampling the aqueous phase (Dearden and Bresnen, 1988; Klein et al., 1988).

2.8. Gastrointestinal stability studies

These studies were performed using simulated gastric fluid (SGF) and simulated intestinal fluid (SIF) according to the USP. SGF contained isotonic solution of 0.32% w/v of pepsin having pH 1.2 (adjusted with HCl). SIF contained 1% w/v pancreatin in phosphate buffer (0.68% w/v monobasic potassium phosphate) of pH 6.8 ± 0.1. Drug solution (1 mM) was incubated with SGF and SIF at 37 °C/60 rpm for 2 h and 3 h respectively. Sampling was done at time interval of 20, 40, 60, 90, 120, 180 min and analyzed using stability indicating HPLC method

2.9. pH stability studies

2.9.1. pH-stability profile

Stability of NP-647 (100 μg mL^{-1}) at pH ranging from 3 to 9 was performed at 60 °C. pH of the solution was adjusted with 0.5 M HCl or 0.5 M NaOH. Samples were withdrawn at time intervals of 1, 2, 4, 8, 16, 24 and 28 days and analyzed by HPLC using stability indicating assay method.

2.9.2. Stability in different buffers

Studies were performed in blank, citrate, tartrate and phosphate buffers. Experiments were performed at pH 3.0, 4.0, 5.0 and 6.0 using 50 mM of each buffer at 80 °C. Ionic strength of the buffers were maintained to 154 mM using NaCl. Samples were withdrawn at time intervals of 1, 2, 4, 8, 16, 24 and 32 days and analyzed by HPLC using stability indicating assay method.

Table 1
Software predictions of log *P*, pK_a and log S_o.

Software	Predicted values		
	log *P*	pK_a	log S_o (M)
ACD/lab	–[a]	6.98	−2.16
ADME/T	−1.37	–[a]	−2.53
Pallas	−0.98	7.05	*[b]
Discovery studio	−1.01	*[b]	−1.28
Vcclab	−0.83	*[b]	−2.48
Average	−1.05	7.02	−2.1

[a] Value is not considered.
[b] Software does not predict value.

2.10. Temperature stability studies

The temperature dependency of NP-647 degradation was tested at 40, 50, 60 and 80 °C. Experiments were performed with 50 μg mL^{-1} drug concentration in tartrate buffer (50 mM) of pH 5.0 and with ionic strength of 154 mM. Samples were withdrawn at time intervals of 1, 2, 3, 4, 5 and 6 weeks and analyzed by HPLC using stability indicating assay method.

3. Results and discussion

3.1. Insilico prediction of physicochemical properties of NP-647

Based on the predicted values of solubility parameters given by five software programs for TRH, three consensus namely, average, median and harmonic mean were developed. It was found that consensus of average was correlated best among three consensus. Models for pK_a, log *P* and solubility prediction consist of average consensus of ACD/lab, Pallas, ADME/Toxes software; Discovery studio, Pallas, ADME/Toxes, VCCLAB software and ACD/lab, ADME/Toxes, Discovery studio, VCCLAB software respectively. These models when used for prediction of NP-647, gave values that were closer to experimentally determined values (r^2 = 0.9999) than any individual software used above (Table 1).

3.2. Solid state characterization

3.2.1. Characterization of solid form of NP-647

NP-647 was identified as an amorphous material by XRPD. Fig. 2 shows halo pattern, characteristic of amorphous material. Amorphous nature of NP-647 was further confirmed by an absence of birefringence as observed in the polarized light microscopy (Fig. 3).

NP-647, when subjected to conventional DSC in a crimped aluminium pan (Fig. 4), showed two endotherms, with maxima at 70 °C and 300 °C respectively. First broad endotherm (from 40 °C to 110 °C), was attributed to the moisture loss (dehydration) of NP-647 which was corresponding to the first step change in TGA trace (Fig. 5). Second endortherm was associated with decomposition and corresponded to the second step change in TGA trace (Fig. 5).

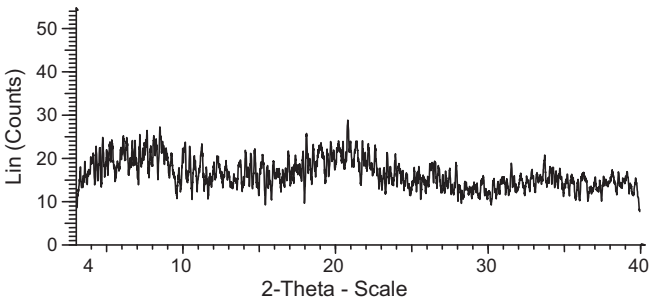

Fig. 2. XRPD diffractograms of NP-647.

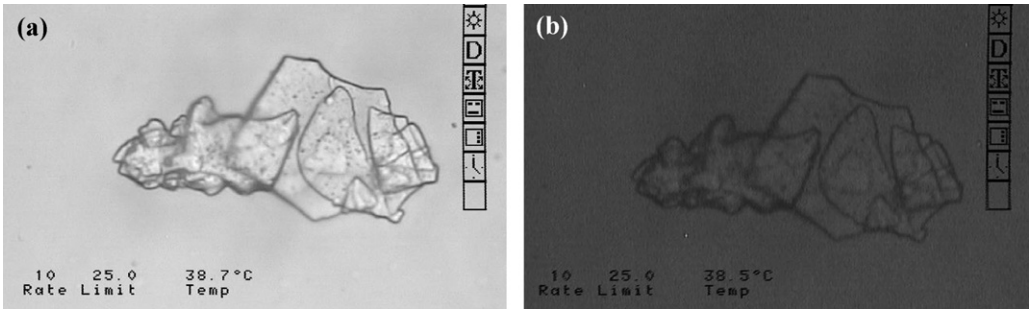

Fig. 3. Microscopic photographs of NP-647.

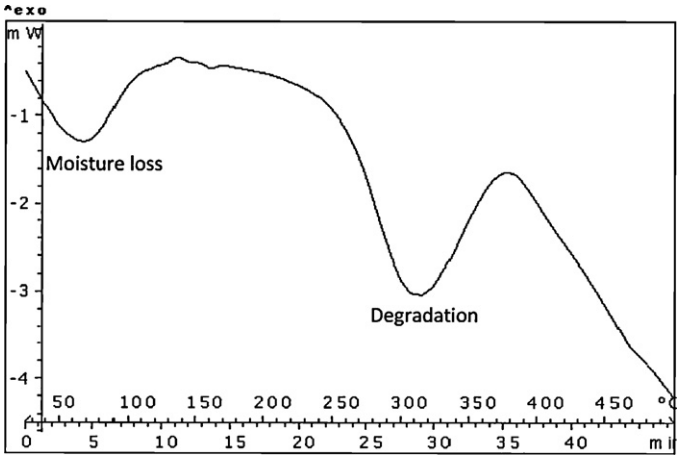

Fig. 4. DSC trace of NP-647.

The endotherm corresponding to the glass transition temperature (T_g) could not be seen in conventional DSC trace. This was probably, because of the overlapping of endothermic events corresponding to the moisture loss and glass transition.

T_g of NP-647 was determined by modulated DSC, using the reversible heat flow signal (Fig. 6(a)), with the accompanying water loss being observed in the non-reversing signal (Fig. 6(b)). Amorphous form of NP-647 was generated *in situ* and T_g was determined. An endotherm corresponding to the glass transition occurred in reversible heat flow at 75.13 °C (onset). High value of T_g indicates its relatively stable amorphous nature.

Fig. 7 shows the MDSC curves for samples equilibrated at 50% RH. The results suggested that in presence of moisture (4.7% characterized by TGA), T_g decreased to 66.73 °C (onset), indicating plasticization by water.

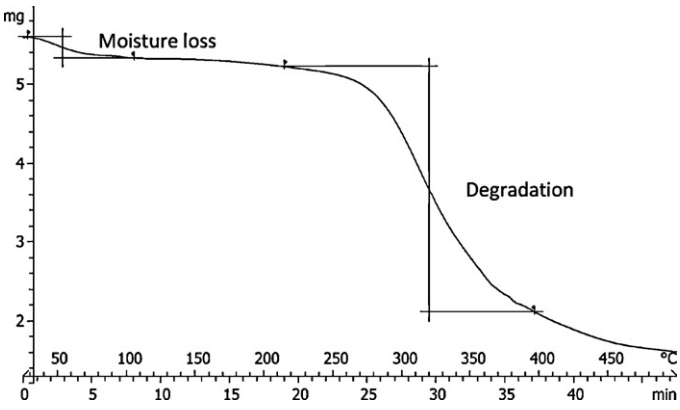

Fig. 5. TGA trace of NP-647.

3.2.2. Sorption–desorption studies on amorphous form of NP-647

Sorption–desorption isotherm of NP-647 is shown in Fig. 8. Desorption curve 1 showed moisture loss by NP-647 when the RH was changed from 25 to 0%. NP-647 absorbed moisture linearly as indicated by sorption curves 1 and 2; hence followed BET type III moisture isotherm. Moisture sorption isotherm showed hysteresis, which is common for amorphous material. At lower RH values (below 40% RH), moisture uptake was relatively low. Probably water uptake mechanism is dominated by surface adsorption only. There was a sharp increase in water sorption above 50% RH, most likely due to bulk absorption mechanism of water sorption. No sharp loss in mass at any RH value was observed, indicating absence of amorphous to crystalline transformation (Burnett et al., 2004). Desorption curve 2 indicated reversible moisture loss, thus confirming no hydrate formation and/or recrystallization.

3.2.3. Hygroscopicity classification of NP-647

Results of sorption studies (Fig. 8) indicated that NP-647 was deliquescent in nature and absorbed more than 15% w/w moisture at 25 °C/80% RH. Hence it can be categorized as a class IV drug (very hygroscopic) according to hygroscopicity classification schemes of European pharmacopeia. Moisture content of NP-647 started increasing at 40 °C and it absorbed more than 20% moisture above 90% RH suggesting very hygroscopic nature according to the criteria of Callahan et al. (1982).

3.2.4. Oral solid form of NP-647 and hygroscopicity

Hygroscopic nature of NP-647 is expected to create problem during handling and processing of its solid dosage forms like tablets and capsules. Moreover NP-647 has very good water solubility; hence amorphous form does not provide any additional advantage for its oral delivery. Moisture sorption behavior of NP-647 is similar to its parent compounds i.e., TRH. In case of TRH, salt formation results in non-hygroscopic crystal form (Fujino and Hatanaka, 1976). Hence to overcome this problem, crystalline salt formation can be explored.

3.3. pK_a determination

pK_a describes the acid/base character of a drug and gives an idea about the charge state of a molecule in solution at a particular pH. This charge state of a molecule plays an important role in absorption, transport and its binding to the receptor (Deák et al., 2008).

3.3.1. Experimental

Electron quality control (EQC) and titrant quality control (TQC) were performed before doing pK_a determination experiments. All the quality control parameters were within their acceptable limits.

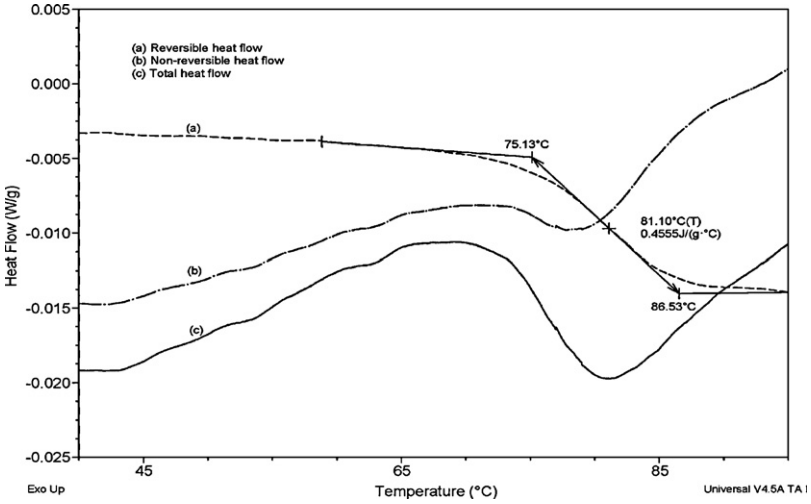

Fig. 6. MDSC trace of *in situ* generated amorphous form of NP-647.

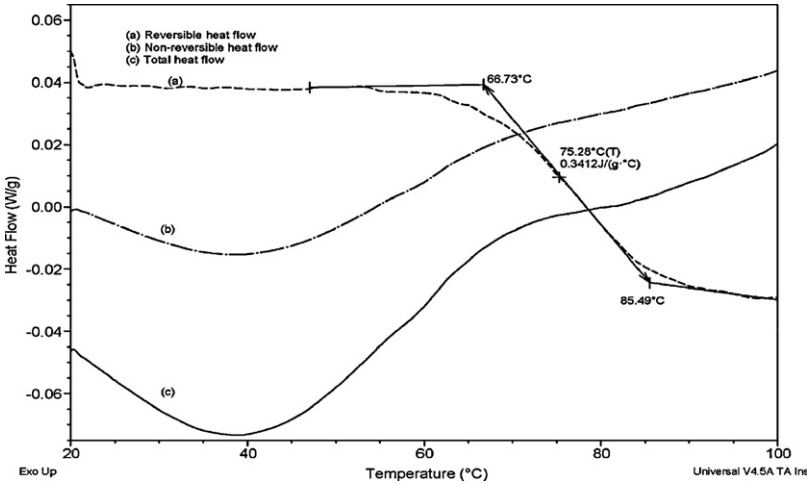

Fig. 7. MDSC trace of NP-647.

pSOL instrument generated the 'simulated titration curve' with the help of the given input (predicted pK_a value). Data of three titrations was refined using pS software of pSOL Gemini (Table 2).

Data refined using pS software generates the titration curve, Bjerrum plot and speciation profile of NP-647 (Fig. 9). Fig. 9(b) shows the Bjerrum plot for titration of NP-647, which indicates only one pK_a value (average number of bound protons per molecule; $\bar{n}_H = 1.0$). Bjerrum plot reveals the pK_a of NP-647 as the pH value at $\bar{n}_H$ of 0.5, i.e., half of the protons being bound to the molecule. Ionization of NP-647 starts below pH of 9.0 as indicated by a rise in $\bar{n}_H$ values. Speciation profile (Fig. 9(c)) shows that the molecule is ionized at low pH, but % ionization decreases with increasing pH. At pH 7.2, both ionized (BH^+) and unionized (B) form of NP-647 equally exist, i.e., pK_a. As the molecule becomes totally unionized at higher pH, solubility of NP-647 above pH 9.0 would be its intrinsic solubility.

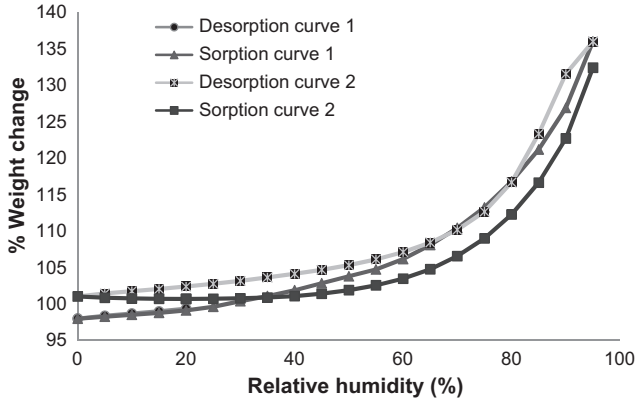

Fig. 8. Sorption isotherm of amorphous form of NP-647.

3.3.2. NP-647 is stronger base than TRH

The basic nature of TRH is attributed to the imidazole ring of the histidine amino acid. Conjugated acid of TRH, thus generated, has a positively charged imidazole ring which is stabilized by ring resonance. NP-647, being a TRH analogue, has similar structure with an imidazole ring, which confers it, a basic nature (Fig. 10(a)); the fact

Table 2
Experimental pK_a values of NP-647.

Titration	pK_a	Average pK_a	Group GOF[a]
1	7.18		
2	7.21	7.2 ± 0.02	1.90
3	7.21		

[a] Goodness of fit.

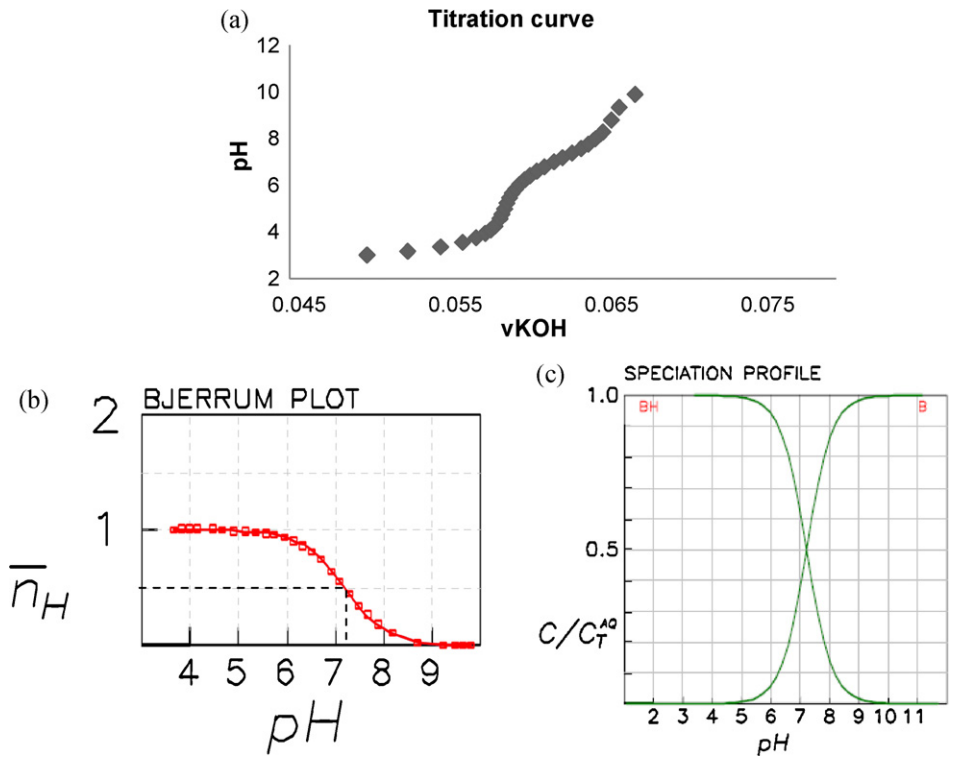

Fig. 9. Graphical representation of dissociation studies (a) titration curve, (b) Bjerrum plot and (c) speciation profile of NP-647.

is also supported by software programs like ACD/I-lab and Pallas. However, NP-647 (pK_a = 7.2) has a pK_a value higher than that of TRH (pK_a = 6.2) (Leonard et al., 2000), which may be due to the presence of electron donating propyl group substitution at C-2 position in the imidazole ring. As shown in Fig. 10(b) and (c), conjugated acid of NP-647 (positively charged imidazole ring) is stabilized by ring resonance as well as a positive inductive effect (+I) of the substituted propyl group, while in case of TRH, only resonance stabilization is present. Thus, conjugated acid formed in case of NP-647, is more stable than that in TRH, making it a stronger base. Other side-chain functional group in the NP-647 including the amide group (neutral) does not contribute to the ionization behavior.

3.4. Solubility studies

As mentioned in Section 2.6.3, simulated titration curve was created before starting the actual dissolution titration by using a pK_a (7.2), log P (−1.07) and a predicted intrinsic solubility (3.24 mg mL^{-1}). In Fig. 11, the anticipated 'precipitation region' is indicated as zone A, while zones B and C indicate the expected dissolution region. Since predicted intrinsic solubility was greater than 0.5 mg mL^{-1}, there was no need of 'pre-dissolution' of samples, which is usually done in the case of the sparingly soluble samples (Avdeef et al., 2000).

In case of NP-647, titration was started from zone 'A' of simulated titration curve i.e., a high pH region. Instrument dispensed the titrant (0.5 M KOH) into the sample to reach the region of precipitation. Subsequently, the pH of slurry was driven in the direction of dissolution zone, by repeatedly dispensing 0.5 M HCl accurately. Zone B (0.8 pH unit above the complete dissolution) was the most important zone for data collection and hence called as "information rich zone". Instrument spent 80% of the total titration time in zone 'B'. Rate of collecting data point was very slow in zone B, moderate in zone 'A' and fast in zone 'C'. Fig. 12(a) shows the Bjerrum plot of the dissolution titration performed with NP-647. The right curve in the plot was calculated by the software of pSOL instrument from the true pK_a value. This curve represents a titration of NP-647 in absence of precipitant (also see Fig. 9(b)). The left curve corresponds to a titration, in which precipitation occurred. As mentioned before, in presence of precipitation, pK_a value of NP-647 was shifted to lower side (Avdeef, 2003)

3.4.1. Refinement of solubility data

Data of each titration was refined using pS software to achieve an acceptable GOF. Table 3 summarizes the data obtained from titration condition, along with the intrinsic solubility constant of NP-647. Solubility profile of NP-647 is shown in Fig. 13.

3.4.2. Biopharmaceutical parameters of NP-647

Three important biopharmaceutical parameters (T_{disso}, D_{abs} and D_n), predicting the *in vivo* performance of NP-647 were calculated using P_{eff} (7.56×10^{-4} cm s^{-1}), ρ (1320 mg cm^{-3}), r (2.5 μm), C_s (11.0 mg mL^{-1} at pH 6.5), D (assumed to be 5×10^{-6} cm^2 s^{-1}), h (assumed to be 0.003 cm), MITT (199 min), and A (800 cm^2) (Rinaki et al., 2003; Yu, 1999).

Dissolution time (T_{disso}) is the minimum time required to dissolve a single particle of the drug under sink condition. NP-647 has a T_{disso} value of 0.1 min indicating that absorption of drug will not be dissolution limited (T_{disso} < 199 min). Absorbable dose (D_{abs}) is the amount of a drug that can be absorbed during the period of gastrointestinal transit when the solution contacting the effective surface area of absorption is saturated with the drug. In case of NP-647, D_{abs} value is 8.45 g, indicating that even high dose of NP-647 shall not have any problems related to the solubility (D_{abs} > $D_{NP\text{-}647}$). NP-647

Table 3
Experimental intrinsic solubility of NP-647.

Titration	log S_o	Average log S_o	Group GOF
1	−2.22		
2	−2.24	−2.23 ± 0.01	6.26
3	−2.22		

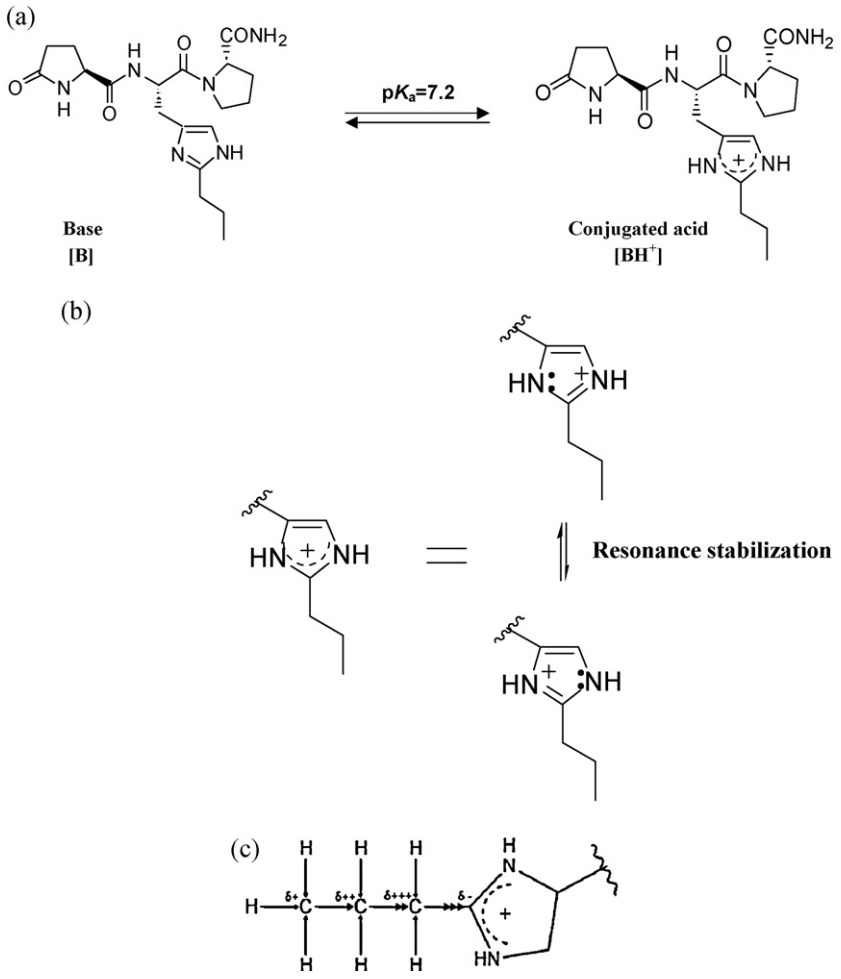

Fig. 10. (a) Ionization of NP-647, (b) resonance stabilization of imidazole ring and (c) inductive effect of propyl group. NP-647 is basic in nature, hence ionized to the corresponding conjugate acid. This positively charged ionized form is stabilized by the ring resonance and positive inductive effect of propyl group.

also has a very high dissolution number, i.e., 1990 min, indicating that drug has an acceptable dissolution profile.

3.5. log *P* and log *D* determination

log *P* i.e., the logarithm of octanol–water/buffer partition coefficient, is one of the best indicator of lipophilicity of a molecule. Its role in drug development is well established and is extensively used in rational drug design (Deák et al., 2008).

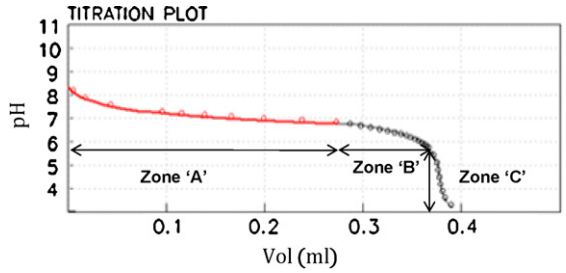

Fig. 11. Simulated titration curve generated by pSOL for NP-647, using a pK_a value of 7.2 and a log *P* of 1.07. Zone 'A' indicates the anticipated 'precipitation region' while zones B and C indicate the expected dissolution region.

3.5.1. Partitioning of NP-647 in n-octanol and aqueous phase

NP-647 has one pK_a and gets ionized in the aqueous phase (pH < 9.0). Therefore, it has two micro species, i.e., unionized [B] and ionized [BH^+] form (Fig. 10). Partition coefficient of the unionized species (neutral form) is indicated by a symbol *P*, while that of ionized species is indicated by P_{+1}. The ratio of the sum of the concentrations of these two species in octanol, to the sum of their concentrations in water, is called the distribution coefficient and is indicated by symbol *D*.

3.5.2. Experimental

Table 4 shows the measured values, log *P* and log $D_{7.4}$ were followed the well-known equation that which relates the log *P* and

Table 4
Experimental log *P* and log *D* of NP-647.

Phase ratio	Partition/distribution coefficient	log *P*/*D*	Mean ± SD
Partition coefficient (log *P*)			
1:1	0.1014	−0.99	
1:2	0.0819	−1.09	−1.07 ± 0.06
2:1	0.0740	−1.13	
Distribution coefficients (log $D_{7.4}$)			
1:1	0.0564	−1.25	
1:2	0.0602	−1.22	−1.24 ± 0.02
2:1	0.0551	−1.26	

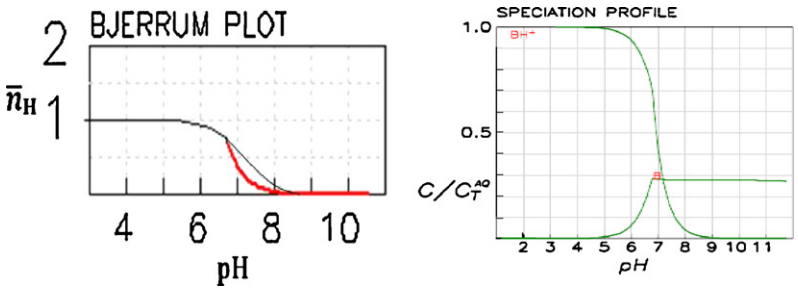

Fig. 12. (a) Bjerrum plot of NP-647 showing shift in pK_a value in presence of precipitation and (b) speciation profile of NP-647 during dissolution titration (DTT method).

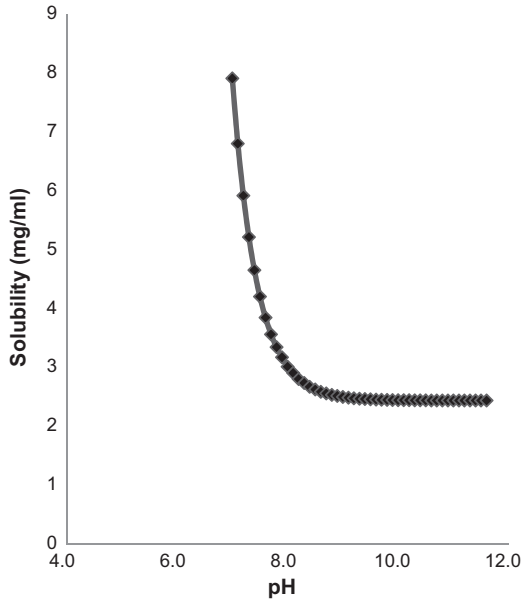

Fig. 13. pH solubility profile of NP-647.

log *D* values for a basic compound.

$$\log D_{pH} = \log P - \log(1 + 10^{pK_a - pH}) \quad (6)$$

Hence, entire log D_{pH} profile can be generated using this equation.

Compared to TRH, NP-647 has a higher partition coefficient, indicating more hydrophobic nature. This increased hydrophobicity may be attributed to the added propyl group at C-2 position of imidazole moiety of NP-647.

3.5.3. log *P* and GI membrane permeability of NP-647

There is a well established correlation between log *P* value of a molecule and bioavailability. Optimum log *P* value for oral absorption is 1.8 (Earll, 1999). Like most of peptides, NP-647 also has a negative log *P* value i.e., −1.07. Hence its oral absorption through passive diffusion will be less. However, most of the peptides cross GI membrane through the peptide transporters (PEPT-1). Caco-2 studies indicated carrier mediated transport of NP-647 across cell monolayer (data not shown).

Many literature reports support active transport of TRH and its analogue across the intestine as well as BBB (Urayama et al., 2003; Walter and Kissel, 1994; Yokohama et al., 1984). Preclinical studies of NP-647 established its antiepileptic activity, providing an evidence for crossing of BBB. A log *P* of 2.7 is required for a molecule to cross BBB by passive diffusion (Earll, 1999). NP-647 crosses BBB despite a negative log *P* value, indicating its active/carrier mediated transport across BBB, like TRH. Further studies are required to investigate its transport mechanism, across the biological membrane.

3.6. Stability studies

3.6.1. Gastrointestinal stability studies

There was no metabolism and/or degradation in SGF and SIF (UPS) for the periods of 2 h and 3 h respectively. Thus, NP-647 was found to be stable in gastrointestinal environment. There is no first pass metabolism of NP-647 (data not shown) and it is also stable in GIT; thus indicating suitability of oral route for its delivery.

3.6.2. pH stability studies

3.6.2.1. pH-stability profile. Degradation of NP-647 decreased as pH increased up to pH 5.0 and after pH 5.0, degradation started increasing as pH increased (Fig. 14). Hence, NP-647 is most stable at pH of 5.0. This finding is also supported by the pH-stability data of TRH and its other analogues which are also stable at the same pH.

3.6.2.2. Stability in different buffers. It is a well established fact that buffer species affect the stability of drug in solution. In case of NP-647, its solution stability varies with different buffer species (Fig. 15). NP-647 was found to be most stable in the tartrate buffer of pH 5.0 (ionic strength 154 mM).

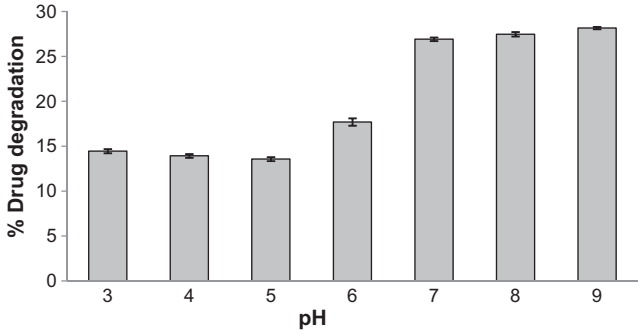

Fig. 14. pH stability profile of NP-647 (28 days data).

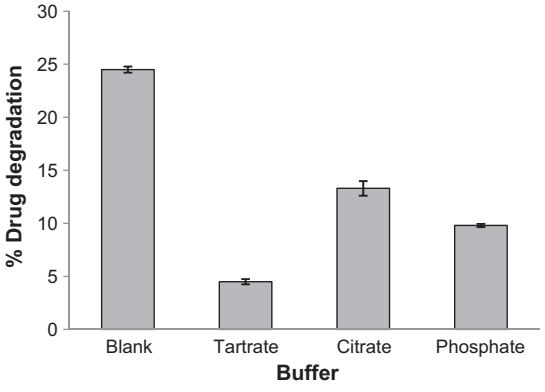

Fig. 15. Stability of NP-647 in different buffers of pH 5.0 (32 days data).

3.6.3. Temperature stability

Over the temperature range of 50–80 °C, degradation of NP-647 followed first order kinetics. Degradation rates of NP-647 increased with increasing temperature. Activation energy (E_a) and Arrhenius factor (A) were determined using Arrhenius plot and were found to be 5.1 kcal/mol and 3.39 day^{-1}, respectively. The extrapolation of the regression curve to 25 °C gave the value of $k_{20} = 6.2 \times 10^{-4}$ day^{-1}. Half life ($t_{0.5}$) and shelf life ($t_{0.9}$) of NP-647 were calculated as 1124 days (3.2 years) and 172 days (~6 months), respectively in tartrate buffer of pH 5.0 solution.

4. Conclusion

As discussed previously, NP-647 is tri-peptide, having promising antiepileptic activity. In case of epilepsy, prolonged treatment is required to control seizure attacks. Hence oral delivery of a drug is preferable. However, in case of emergency, for example, status epilepticus or intractable epilepsy, parenteral administration is required.

Despite its peptide nature, NP-647 is stable toward pH as well as enzymatic degradation in gastrointestinal track. Values of solubility parameters as well as biopharmaceutical parameters (T_{disso}, D_{abs} and D_n) indicate that NP-647 can be given orally and its bioavailability will neither dissolution nor solubility rate limited. However, hygroscopicity will lead to the process related problems in its solid dosage formulation. As the case of other amorphous compound, it may undergo devitrification. Since water has plasticizing effect, humidity control will be very critical during its processing. Solubility, lipophilicity and solution stability studies of NP-647 indicated that there will not be any problem for its parenteral delivery.

Solubility parameters like pK_a, intrinsic solubility and partition coefficient play a vital role in the formulation development of a new chemical entity. Hence accurate prediction of these parameters helps in drug discovery and development. Consensus approach used gave values that were closer to experimentally determined values ($r^2 = 0.9999$) than any individual software. Further studies are necessary for validation of these models.

Acknowledgements

Lokesh Kumar acknowledges Department of Science and Technology (DST), Govt. of India for providing Senior Research Fellowship. Authors would also like to thank TA Instruments, Bangaluru (India) for performing vapor sorption analysis.

References

Abshear, T., Banik, G.M., D'Souza, M.L., Nedwed, K., Peng, C., 2006. A model validation and consensus building environment. SAR QSAR Environ. Res. 17, 311–321.
Albert, M., Jenike, M., Nixon, R., Nobel, K., 1993. Thyrotropin response to thyrotropin-releasing hormone in patients with dementia of the Alzheimer type 1. Biol. Psychiatry 33, 267–271.
Amidon, G.L., Lennernäs, H., Shah, V.P., Crison, J.R., 1995. A theoretical basis for a biopharmaceutic drug classification: the correlation of *in vitro* drug product dissolution and *in vivo* bioavailability. Pharm. Res. 12, 413–420.
Avdeef, A., 1998. pH-metric solubility. 1. Solubility-pH profiles from Bjerrum plots. Gibbs buffer and pK_a in the solid state. Pharmacol. Res. Commun. 4, 165–170.
Avdeef, A., 2003. Absorption and Drug Development: Solubility, Permeability and Charge State. John Wiley & Sons, Inc., New Jersey.
Avdeef, A., Berger, C.M., 2001. pH-metric solubility. 3. Dissolution titration template method for solubility determination. Eur. J. Pharm. Sci. 14, 281–291.
Avdeef, A., Berger, C.M., Brownell, C., 2000. pH-metric solubility. 2: correlation between the acid–base titration and the saturation shake-flask solubility-pH methods. Pharm. Res. 17, 85–89.
Burnett, D.J., Thielmann, F., Booth, J., 2004. Determining the critical relative humidity for moisture-induced phase transitions. Int. J. Pharm. 287, 123–133.
Callahan, J.C., Cleary, G.W., Elefant, M., Kaplan, G., Kensler, T., Nash, R.A., 1982. Equilibrium moisture content of pharmaceutical excipients. Drug Dev. Ind. Pharm. 8, 355–369.
Deák, K., Takács-Novák, K., Kapás, M., Vastag, M., Tihanyi, K., Noszál, B., 2008. Physico-chemical characterization of a novel group of dopamine D3/D2 receptor ligands, potential atypical antipsychotic agents. J. Pharm. Biomed. Anal. 48, 678–684.
Dearden, J., Worth, A., 2007. *In silico* prediction of physicochemical properties. JRC Sci. Tech. Rep., 1–73.
Dearden, J.C., Bresnen, G.M., 1988. The measurement of partition coefficients. Quant. Struct.–Act. Relat. 7, 133–144.
Earll, M., 1999. A Guide to log P and pK_a Measurements and Their Use. http://www.raell.demon.co.uk/chem/logp/logppka.htm, Accessed: 24/2/2010.
Ford, H., Merski, C.L., Kelley, J.A., 1991. Rapid microscale method for the determination of partition coefficients by HPLC. J. Liq. Chromatogr. Related Technol. 14, 3365–3386.
Fujino, M., Hatanaka, C., 1976. TRH tartrate crystals. U. S. Patent 3959247.
Griffith, E., 1985. Thyrotropin releasing hormone: endocrine and central effects. Psychoneuroendocrinology 10, 225–235.
Heuer, H., Schafer, M.K.H., O'Donnell, D., Walker, P., Bauer, K., 2000. Expression of thyrotropin-releasing hormone receptor 2 (TRH-R2) in the central nervous system of rats. J. Comp. Neurol. 428, 319–336.
ICH, 1996. Validation of analytical procedures: text and methodology. In: Proceeding of the International Conference on Harmonisation , Geneva.
Jain, R., Kaur, N., Monga, V., 2006. CNS effective thyrotropin releasing hormone analogs. WTO Indian Patent Application No. 2065/DEL/2006.
Jaworska-Feil, L., Kajta, M., Budziszewska, B., Lekiewicz, M., Laso, W., 2001. Protective effects of TRH and its stable analogue, RGH-2202, on kainate-induced seizures and neurotoxicity in rodents. Epilepsy Res. 43, 67–73.
Kaur, N., Lu, X., Gershengorn, M.C., Jain, R., 2005. Thyrotropin-releasing hormone (TRH) analogues that exhibit selectivity to TRH receptor subtype 2. J. Med. Chem 48, 6162–6165.
Kaur, N., Monga, V., Lu, X., Gershengorn, M.C., Jain, R., 2007. Modifications of the pyroglutamic acid and histidine residues in thyrotropin-releasing hormone (TRH) yield analogs with selectivity for TRH receptor type 2 over type 1. Bioorg. Med. Chem. 15, 433–443.
Klein, W., Kördel, W., Weiss, M., Poremski, H.J., 1988. Updating of the OECD test guideline 107 "partition coefficient n-octanol/water": OECD laboratory intercomparison test on the HPLC method. Chemosphere 17, 361–386.
Kubek, M.J., Garg, B.P., 2002. Thyrotropin-releasing hormone in the treatment of intractable epilepsy. Pediatr. Neurol. 26, 9–17.
Lafer, B., Fava, M., Hammerness, P., Rosenbaum, J.F., 1993. The influence of DST and TRH test administration on depression assessments: a controlled study. Biol. Psychiatry 34, 650–653.
Leonard, M., Creed, E., Brayden, D., Baird, A.W., 2000. Iontophoresis-enhanced absorptive flux of polar molecules across intestinal tissue in vitro. Pharm. Res. 17, 476–478.
Nemeroff, C.B., Widerlov, E., Bissette, G., Walleus, H., Karlsson, I., Eklund, K., Kilts, C.D., Loosen, P.T., Vale, W., 1984. Elevated concentrations of CSF corticotropin-releasing factor-like immunoreactivity in depressed patients. Science 226, 1342–1344.
O'Leary, R., O'Connor, B., 1995. Thyrotropin-releasing hormone. J. Neurochem. 65, 953–963.
Rajput, S.K., Krishnamoorthy, S., Pawar, C., Kaur, N., Monga, V., Meena, C.L., Jain, R., Sharma, S.S., 2009. Antiepileptic potential and behavioral profile of L-pGlu-(2-propyl)-L-His-L-ProNH2, a newer thyrotropin-releasing hormone analog. Epilepsy Behav. 14, 48–53.
Rathore, R., Jain, J.P., Srivastava, A., Jachak, S.M., Kumar, N., 2008. Simultaneous determination of hydrazinocurcumin and phenol red in samples from rat intestinal permeability studies: HPLC method development and validation. J. Pharm. Biomed. Anal. 46, 374–380.
Rinaki, E., Valsami, G., Macheras, P., 2003. Quantitative biopharmaceutics classification system: the central role of dose/solubility ratio. Pharm. Res. 20, 1917–1925.
Spindel, E.R., Pettibone, D.J., Wurtman, R.J., 1981. Thyrotropin-releasing hormone (TRH) content of rat striatum: modification by drugs and lesions. Brain Res. 216, 323.
Sun, Y., Lu, X., Gershengorn, M.C., 2003. Thyrotropin-releasing hormone receptors-similarities and differences. J. Mol. Endocrinol. 30, 87–89.
Sun, Y., Zupan, B., Raaka, B.M., Toth, M., Gershengorn, M.C., 2009. TRH-receptor-type-2-deficient mice are euthyroid and exhibit increased depression and reduced anxiety phenotypes. Neuropsychopharmacology 34, 1601–1608.
Takeuchi, Y., Miyanomae, Y., Komatsu, H., Oomizono, Y., Nishimura, A., Okano, S., Nishiki, T., Sawada, T., 1994. Efficacy of thyrotropin-releasing hormone in the treatment of spinal muscular atrophy. J. Child Neurol. 9, 287–292.
Tsuboyama, G.K., Gabriel, S.S., Davis, B.M., Davidson, M., Lawlor, B.A., Ware, K., Davis, K.L., Mohs, R.C., 1992. Neuroendocrine dysfunction in Alzheimer's disease: results following TRH stimulation 1. Biol. Psychiatry 32, 195–198.
Urayama, A., Yamada, S., Ohmori, Y., Deguchi, Y., Uchida, S., Kimura, R., 2003. Blood–brain permeability of [^{3}H]-(3-methyl-His2) thyrotropin-releasing hormone (MeTRH) in mice: effects of TRH and its analogues. Drug Metab. Pharmacokinet. 18, 310–318.
Walter, E., Kissel, T., 1994. Transepithelial transport and metabolism of thyrotropin-releasing hormone (TRH) in monolayers of a human intestinal cell line (Caco-2): evidence for an active transport component? Pharm. Res. 11, 1575–1580.
Yokohama, S., Yamashita, K., Toguchi, H., Takeuchi, J., Kitamori, N., 1984. Absorption of thyrotropin-releasing hormone after oral administration of TRH tartrate monohydrate in the rat, dog and human. J. Pharm. Dyn. 7, 101–111.
Yu, L.X., 1999. An integrated model for determining causes of poor oral drug absorption. Pharm. Res. 16, 1883–1887.